Desalination and Water Treatment
www.deswater.com

doi: 10.1080/19443994.2014.968903

56 (2015) 2567–2575
December

Taylor & Francis
Taylor & Francis Group

Experimental investigation of neutralization dialysis in three-compartment membrane stack

M. Chérif[a,b], I. Mkacher[a], R. Ghalloussi[a], L. Chaabane[a], A. Ben Salah[b], K. Walha[b], L. Dammak[a,*], D. Grande[a]

[a]*Institut de Chimie et des Matériaux Paris-Est (ICMPE), UMR 7182 CNRS—Université Paris-Est, 2 Rue Henri Dunant, 94320 Thiais, France, Tel. +33 149781173; Fax: +33 145171721; email: cherif_mona@hotmail.fr (M. Chérif), Tel. +33 149781173; Fax: +33 149781166; emails: ines.mkacher@gmail.com (I. Mkacher), rim.ghalloussi@yahoo.fr (R. Ghalloussi), lobna.chaabane@u-pec.fr (L. Chaabane), dammak@u-pec.fr (L. Dammak), Tel. +33 149781177; Fax: +33 149781166; email: grande@icmpe.cnrs.fr (D. Grande)*
[b]*Laboratoire des Sciences des Matériaux et de l'Environnement, Université de Sfax, Route de Soukra km 4-BP 1171, Sfax 3000, Tunisia, Tel. +216 98414168; Fax: +216 74674810; email: abdelhamid.bensalah@fss.rnu.tn (A. Ben Salah), Tel. +216 27983966; Fax: +216 74674810; email: walha.khaled@yahoo.com (K. Walha)*

Received 10 December 2013; Accepted 28 May 2014

ABSTRACT

This work is concerned with the feasibility of surface water desalination by the neutralization dialysis (ND) process and the difficulties related to it. The pH and the conductivity of model saline solution have been measured during different ND operations, using a three-compartment membrane stack of 64 cm^2 active area for each ion-exchange membrane (IEM). The saline solution concentration is maintained at 0.02 $mol\,L^{-1}$. The influence of three parameters has been investigated, i.e. the flow rate (from 35 to 100 $mL\,min^{-1}$), the alkaline solution concentration, and the acidic solution concentration (from 0.02 to 0.1 $mol\,L^{-1}$). We have shown that diffusion boundary layers have a great influence on the ion-exchange kinetics through the IEMs. A leakage of HCl solution through the cation-exchange membrane has been proved. Its influence is more pronounced when the acidic and alkaline solution concentrations are low. These leakages modify the shapes of the pH vs. time and conductivity vs. time curves, and decelerate the desalination efficiency. After 2–3 h of desalination process, the conductivity reached the value of 0.25 $mS\,cm^{-1}$, as recommended by the Organisation Mondiale de la Santé (OMS) for a drinking water. The desalination process was achieved within a reasonable duration in all the experiments.

Keywords: Ion-exchange membrane; Neutralization dialysis; Desalination; Surface water

1. Introduction

For many years, water was considered as a free and inexhaustible natural resource. However, prospecting studies reveal an alarming decrease in water reserves in the next 25 years. In some countries such as certain countries of Mediterranean Basin, drinking water needs exceeds the natural resources reserve. The main drinking water resources are the

---

*Corresponding author.

Presented at the 4th Maghreb Conference on Desalination and Water Treatment (CMTDE 2013)
15–18 December 2013, Hammamet, Tunisia

ground water and the surface water. The surface water is an accessible and renewable resource but is easily polluted and contains 1–8 g L^{-1} of salts. However, the ground water is less accessible and is not a renewable resource. Thus, the surface water desalination process can be a viable solution to reduce the effect of drinking water rarefaction, produce drinking water, and satisfy the water needs. The increasing salt amount in the surface water is mainly due to industrial effluents, [1] massive agriculture exploitation, [2] and human pollution [3]. A high NaCl concentration in surface water can have a negative impact on the aquatic ecosystem [4,5] and on human health. Indeed, drinking saline water can cause serious illnesses such as renal problems, cervical cancer, and high blood pressure. Different water desalination processes were carried out or under study [6–9]. One of the most promising techniques is the neutralization dialysis (ND). Indeed, this process consumes low energy and is relatively easy to install. ND is a membrane process suggested first by Igawa et al. [10] in 1987, as a new water desalination method. It is an energy-saving process that uses ion-exchange membranes (IEMs) based on the simultaneous use of two Donnan dialysis operations. In this process, the saline solution is placed between an acidic solution and an alkaline solution separated by cation-exchange membrane (CEM) and anion-exchange membrane (AEM), respectively. The CEM and AEM allow the substitution of cations (anions) of the treated solution by H^+ (OH^-) ions. Thus, mineral charge of the treated solution decreases and its volume increases, which reduces the concentration of salts and leads to desalinated solution (DS) under ideal conditions. The main advantage of ND rather than electrodialysis (ED) process [11–14] is its lower energy consumption.

The aim of this study is to optimize the ND desalination process conditions, in particular by adjusting the flow rate, and the acid and alkali initial concentrations. This work reveals the influence of flow rate and concentration of the water desalination using ND process.

2. Experimental

2.1. Membrane treatment

In this work, two homogeneous membranes (Neosepta® CMX and AMX, Japan) were used. The CEM, CMX, contains sulfonate groups, whereas the AEM, AMX, contains quaternary ammonium groups. Prior to any membrane process, the IEMs were treated, following with the French standard NF X 45-200 to remove the manufacturing process impurities [15]. This treatment was allowed for the stabilization of the physico-chemical properties, and thus reproducible initial conditions were achieved. This procedure is described in Table 1. The treatment cycle was repeated twice for each membrane.

After these cycles, AMX and CMX were stored in 0.1 M HCl and 0.1 M NaCl, respectively.

2.2. Membrane characterization

For each membrane, the active surface area was equal to 64 cm^2. The main physico-chemical characteristics of the cationic and anionic membranes are shown in Table 2.

2.2.1. Ion-exchange capacity

The ion-exchange capacity is a parameter corresponding to the functional sites per gram of the dry membrane. This parameter was determined by following the French standard NF X 45-200. The counter-ions were forced to transfer to a determined solution with the purpose of titrating them. Samples of 10 cm^2 were immersed into 0.1 M HCl (the counter-ion is Cl^-) for 2 h, then rinsed in ultra pure water, immersed in 1 M HNO_3 for at least 12 h, and the chloride content was determined immediately after. Samples were eventually vacuum dried at 40˚C for 24 h to determine the dry mass.

2.2.2. Water content

The membrane samples, previously immersed in the appropriate stabilization solution, were placed between two foils of filter paper and pressed slightly in order to remove the excess liquid. Then, the membranes were immediately placed in a HB43-S Mettler-Toledo moisture thermobalance in which they were heated to 140˚C, until their mass did not vary (at 0.001 g) for 10 min. The water content (W) was determined by the mass difference between the hydrated (W_a) and the dried (W_b) samples as follows:

$$W\ (\%) = \frac{W_{a-}W_b}{W_b} \times 100$$

2.2.3. Thickness

The membrane thickness (T_m) was measured using a Käfer thickness dial gauge, specially devised for plastic film thickness measurements with 1 μm

Table 1
Treatment cycles associated with AMX and CMX membranes

Membranes	AMX		CMX	
Operations	Solution	Duration (min)	Solution	Duration (min)
1	0.1 M HNO_3	60	0.1 M HCl	60
2	Distilled water	±2	Distilled water	±2
3	0.1 M HCl	60	0.1 M NaOH	60
4	0.1 M NaCl	±2	0.1 M NaCl	±2

Table 2
Main physico-chemical characteristics of CMX and AMX membranes

Membranes	CMX	AMX
Ion-exchange capacity (meq g^{-1})	1.6	1.3
Water content (%)	25	26
Thickness (μm)	170	140
Membrane conductivity (ms cm^{-1})	1.4	3.3

resolution. The membrane thickness value was averaged from measurements at 10 different locations on the effective surface region of the membrane.

2.2.4. Membrane conductivity

The electrical conductivity measurements were carried out using the differential method [16,17]. The experimental assembly used consisted of a clip-type cell at an AC frequency of 10 kHz to measure the membrane conductivity, a conductivity meter CDM92 (Radiometer-Tacussel), and a water bath at 25 ± 0.2°C.

The determination of membrane conductance G_m needed two measurements, one without the membrane (G_1) and another one with the membrane (G_2), to deduce the value:

$$G_m = \frac{G_1 G_2}{G_1 - G_2}$$

Using the values of the membrane thickness (T_m) and the electrode section area ($A = 1\ cm^2$), the membrane conductivity was calculated as:

$$k_m = G_m \times \frac{T_m}{A}$$

The conductivity of CMX and AMX was measured in NaCl solutions at 2×10^{-2} mol L^{-1}.

2.3. ND process

ND operations were performed using a PCCell ED 64-004 electrodialysis stack with three compartments (noted A for acid compartment, B for alkali compartment, and C for saline compartment). The width of each compartment is 450 μm, corresponding to Nylon® spacer thickness. In all the experiments, HCl solution was used in the A compartment and NaOH for the B compartment. For the C compartment, we used a model solution prepared from NaCl, which is referred to as the saline solution. Masterflex® pumps are used to ensure the fluid circulation through the three compartments. It is about a closed circuit.

As shown in Fig. 1, representing a typical ND schema, CMX membrane separates A and C compartments and AMX membrane separates B and C compartments.

In all the experiments, the *A* and *B* circulating solution volumes were 1.5 L and the *C* solution volume was 0.5 L. The differences between solution volumes allow the reduction in the desalination duration. The temperature of each solution is maintained constant at 25.0 ± 0.1 C. After each dialysis operation, the electrodialysis cell was washed with distilled water to remove any impurities present in the spacers (that could come from previous operation).

During the desalination process, the pH and conductivity values were continuously measured in the *C* solution up to 3 h, using a pH meter PHM210 and a conductivity meter CDM92, respectively. The Cl^- and Na^+ final concentrations in the saline compartment were determined by the titration method and flame emission spectrometry, respectively.

The same saline solution was maintained in all of this study. Its main characteristics are: a pH value of 5.5–6.0 and an ion conductivity of 2.0–2.3 mS cm^{-1} at 25°C, which corresponds to an equivalent NaCl concentration of 0.02 mol L^{-1} (1.2 g L^{-1}), significantly higher than the value recommended by the OMS (0.25 mS cm^{-1}) [18].

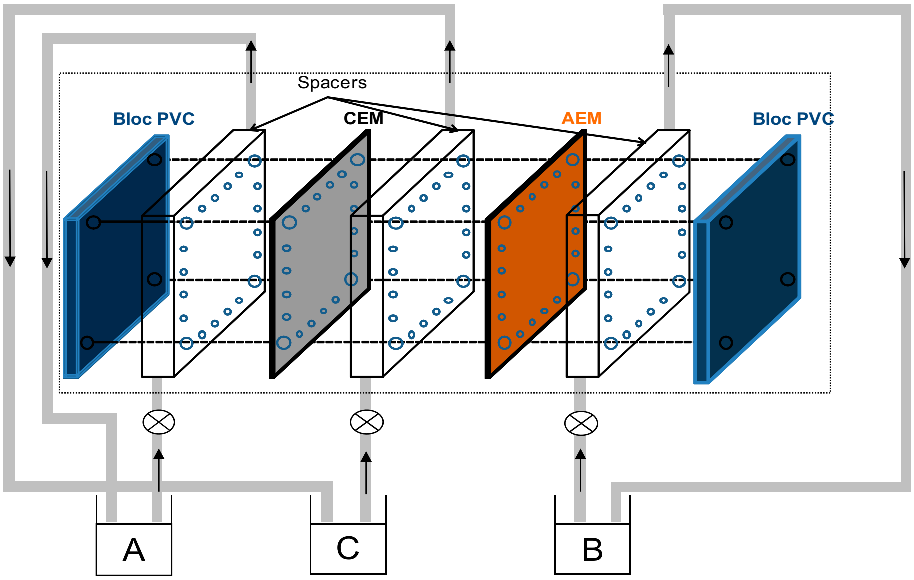

Fig. 1. ND process of model NaCl solution. CEM; AEM; A: acid solution; C: saline solution; B: alkali solution.

3. Results and discussion

In this preliminary study, we investigated the single effect of a certain number of parameters on the ND desalination process. The selected parameters are the initial concentrations of the acidic and alkaline solutions and the alimentation flow rate of the three compartments. The set of the experimental conditions are presented in Table 3.

The experiments numbering in Table 3 will be used for a simple presentation of our results. For example, 1.1 experiment corresponds to $[HCl]_0 = 0.1$ mol L^{-1}, $[NaOH]_0 = 0.1$ mol L^{-1}, and $Q_0 = 35$ mL min^{-1}.

3.1. Effect of flow rate

In the first set of experiments (see 1.1, 1.2, and 1.3 in Table 3), the flow rate effect was investigated, and the fixed concentrations of acid and base solutions were being equal to 0.1 mol L^{-1}. The pH and ion conductivity measured in the saline compartment, during the desalination process are presented in Fig. 2(a) and (b), respectively.

The pH vs. time plots in Fig. 2(a) shows three main stages. First, pH decreases quasi-immediately to acidic values (phase I). Then, a transition through the neutral value to alkaline pH is observed (phase II). The transition is very rapid, i.e. in about 10 min, the pH value progresses from 3 to 10. Finally, a slow pH decrease is observed (phase III). In the 1.2 and 1.3 experiments, the duration of the third phase is about 100 min, and a neutral value of pH (about 7) is attained. However, in the 1.1 experiment, for more than 150 min, the pH values vary slowly from 10 to 9. The pH transitions are accelerated by the rate flow augmentation. This acceleration is due to thinner diffusion boundary layers (DBLs) [19–22] as the flow rate increases. Indeed, the turbulences are created by spacers at the membrane–solution interface. These turbulences lead to thinner DBLs and more important exchange kinetics.

pH vs. time curves show that ion exchanges through IEMs are very sensitive to the use of H^+ and OH^- ions. These two ions are known for their high mobilities both in solutions and in membrane materials with a greater mobility for H^+. Thus, at the beginning of the ND operation, the driving force through the CEM (due to concentration gradients of H^+ and Na^+) must be greater than that through the AEM (due to concentration gradients of OH^- and Cl^-). Therefore, HCl leakage takes place through the CEM and the pH quickly drops from a value close to six to a value close to three (phase I). The presence of H^+ and the progressive demineralization of this saline solution reduce the concentration gradient of H^+ through the CEM and adjust the ion exchanges. Once the demineralization is advanced, and the leakage of H^+ through the CEM actually becomes negligible, NaOH leakage through the AEM increases sharply, and therefore, there is a neutralization reaction of the saline solution corresponding to the phase II of the pH vs. time curves. Rapid and vertical pH variations and a pH equal to seven for the equivalent point confirms this neutralization reaction (phase II). Once the pH become

Table 3
Experimental conditions of ND operations

Experiments		Compartment A C_A = $[HCl]_0$ (mol L^{-1})	Compartment B C_B = $[NaOH]_0$ (mol L^{-1})	Q_0 (mL min^{-1})
1	1	0.1	0.1	35
	2			70
	3			100
2	1	0.05	0.05	70
	2	0.02	0.02	
3	1	0.05	0.05	100
	2	0.02	0.02	
4	1	0.02	0.05	70
	2	0.05	0.02	

alkaline (close to 10), the H^+ ions resume their leakage through the CEM but with a much slower rate because, the concentration gradients of H^+ and Na^+ becomes very weak (demineralization is almost complete). The decrease in pH (phase III) is slow and depends on several parameters such as the demineralization rate at the end of phase II, and the concentration of H^+ ions remaining in the compartment A.

Denisov et al. [23], one of the very few authors in the literature who studied the ND process, used a three-compartment laboratory cell similar to our cell (HCl//NaCl//NaOH) with a 5.5 cm^2 active surface area and a flow rate of 10 mL min^{-1}. These authors tested two kinds of IEMs, i.e. heterogeneous and homogeneous ones, where the pH effect was presented in the case of 0.1 and 0.01 mol L^{-1} initial concentrations of the saline solution. During their experimental studies, Denisov varied the saline solution concentration and fixed all the other parameters such as the acid and alkaline solutions concentration (0.1 mol L^{-1}) as well as the solution flow rates (0.16 mL s^{-1} equivalents to 6.6 mL min^{-1}: an order of magnitude less than that used in this study). Besides, the membrane exchange area was equal to 5.5 cm^2 (almost 12 times less than that used in this study), which is the reason why this author has not observed the third phase of pH curves vs. time. In addition, Denisov did not present the evolution of saline solution conductivity during the desalination process.

The pH curves obtained by Denisov are presented in Fig. 3. Denisov et al. [23] obtained, for concentrations equal to 0.1 mol L^{-1}, a pH decrease that is consistent with the beginning of our pH vs. time curves (phase I) and a pH increase for concentrations equal to 0.01 mol L^{-1}. However, the operating conditions used by these authors did not achieve the other phases (II and III) of the pH evolution within reasonable durations (3 h).

On the other hand, at lower concentration, they observed an increase in pH values (see experimental points: ○). However, at higher concentration, the pH values decrease (see experimental points: ●). Solid curves 1, 2, and 3 show results calculated from two models:

Model 1: ($I \geq 0.1$ mol L^{-1}) the presence of DBLs is neglected. Here, curve 1 corresponds to a $[NaCl]_0$ = 0.1 mol L^{-1}.

Model 2: ($I \leq 0.1$ mol L^{-1}), the effect of the DBLs is assumed to be important. Here, curves 2 and 3 correspond to $[NaCl]_0$ = 0.1 and 0.01 mol L^{-1}, respectively.

Denisov et al. [23] have developed two theoretical models simulating the ion transport through the two IEMs in ND operations. In one case, they have neglected the presence of the DBLs, and in the other case, they took them into account. The results of these two models are presented in Fig. 4. It is noteworthy that our results fit relatively well with those resulting from model 2, i.e. that taking into account the DBLs. However, this model does not explain the pH decrease in the final step. In addition, this model does not provide the theoretical evolution of the saline solution conductivity.

Fig. 2(b) shows the evolution of the saline solution conductivity as a function of time for different flow rates (see experiments 1.1, 1.2, and 1.3 in Table 3). We note for each of the three curves that conductivity values remain quasi-constant at the beginning of desalination (for about 20 min) and then decrease gradually. At the end of desalination process, the conductivity values are about 0.002 mS cm^{-1}, which corresponds to a desalination rate equal to 99.9% and the Cl^- and Na^+ final concentrations in the saline compartment are about 2.4–2.6 × 10^{-4} mol L^{-1} (corresponding to 0.01 g L^{-1}). Thus, we can consider that the desalination is achieved, as the conductivity of drinking water should be between 0.5 and 0.05 mS cm^{-1} according to

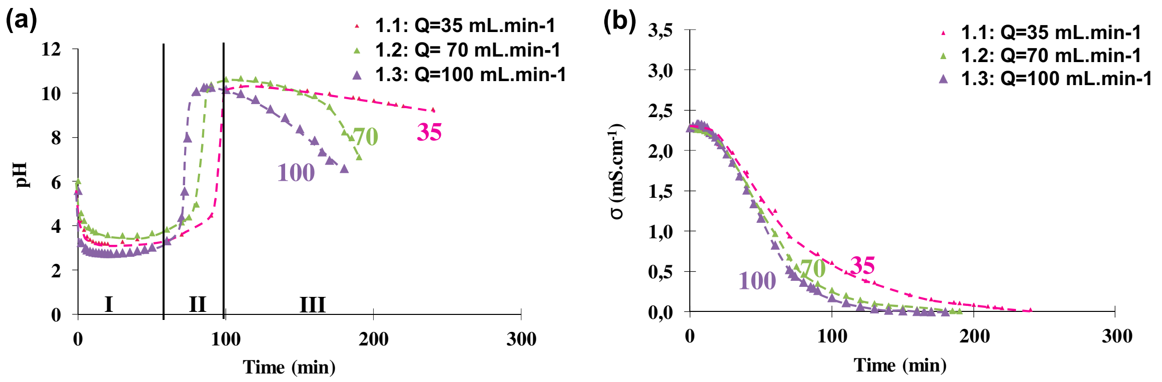

Fig. 2. Effect of flow rate on pH vs. time (a) and saline solution conductivity vs. time (b) plots. $C_A = C_B = 0.1$ mol L^{-1} and $Q_0 = 35$, 70, or 100 mL min^{-1}.

the OMS standards [18]. No noticeable difference is observed between the conductivity values of the 1.2 and 1.3 experiments. The decrease in conductivity values for the 1.1 experiment is slower.

3.2. Effects of acidic and alkaline solution concentrations

In the second set of experiments (see 1.2, 2.1, and 2.2 in Table 3), the effects of acidic and alkaline solution concentrations are investigated. We have chosen to work with high flow rates in order to reduce the DBLs' effects. At high flow rate (70 and 100 mL min^{-1}), the conductivity evolution is quasi-similar. Thus, the flow rate value was fixed at 70 mL min^{-1} for the second experiment set. The pH and saline solution conductivity measured during the desalination process are presented in Fig. 5(a) and (b), respectively. These figures show a behavior similar to that observed in Fig. 2(a) and (b). In this second experiment set, the amplitudes and desalination time are sensitive to the acid and alkali concentrations. Indeed, the ion-exchange kinetics is faster when the acidic and alkaline solution concentrations are higher. The effect of HCl solution leakage through the CEM seems to be higher in low concentrations of acid and alkali solutions. This is confirmed by the shapes of pH vs. time and conductivity σ vs. time curves.

The presence of a concavity in the conductivity curves of the saline solution confirms the presence of

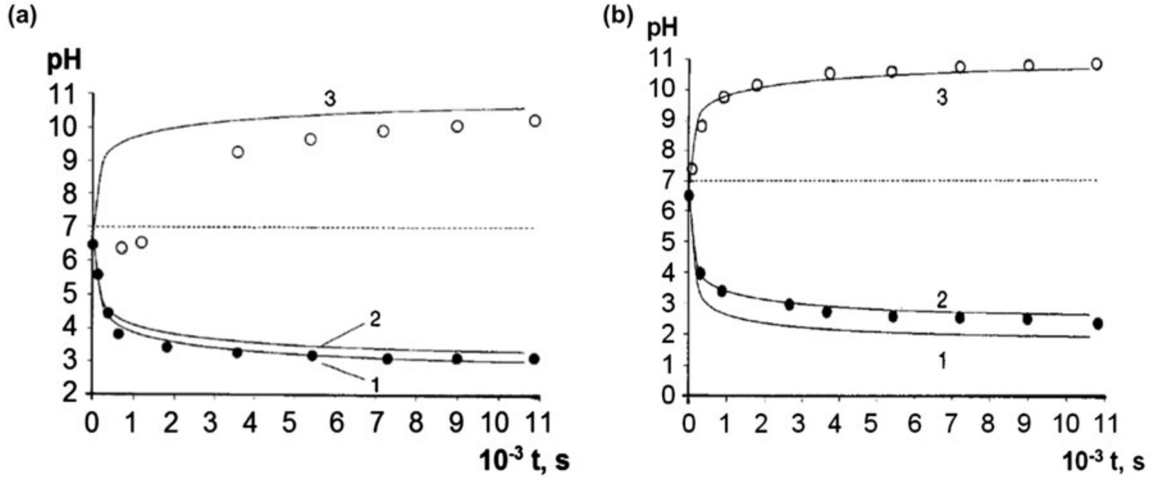

Fig. 3. Time dependence of pH values during the desalination for heterogeneous membranes (a) and homogeneous ones (b) at different initial DS concentrations: (●) 0.1 mol L^{-1}, (○) 0.01 mol L^{-1}. Curves 1, 2, and 3 show results calculated from model 1 (curve 1) and model 2 (curves 2 and 3), respectively. Initial NaCl concentration: (1 and 2) 0.1 mol L^{-1}, (3) 0.01 mol L^{-1} [23].

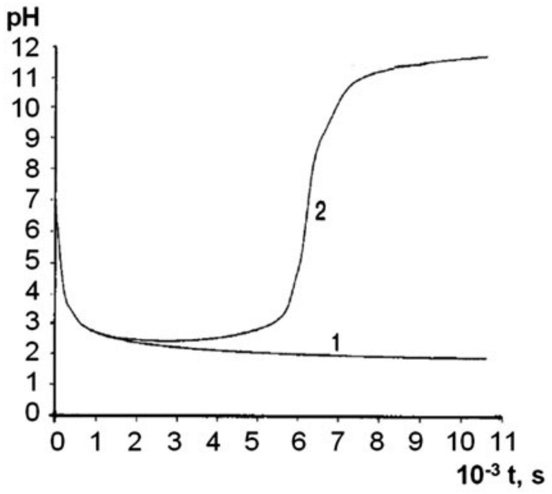

Fig. 4. Theoretical models simulating the NaCl solution desalination by homogeneous membranes where the DBLs are neglected (curve 1) and not neglected (curve 2) [22].

two competing phenomena: (i) HCl solution leakage through the CEM increases the conductivity of the saline solution and (ii) continuous desalting of the saline solution which reduces its conductivity. The compensation of these two phenomena may take about 1 h for low concentrations.

In the third set of experiments (see 1.3, 3.1, and 3.2 in Table 3), we used the same concentrations as in the second experiment set, and we only changed the flow rate to 100 mL min^{-1}. The results obtained with the second and third sets (70 and 100 mL min^{-1}) are presented in Fig. 6(a) and (b). Thus, we can remark that pH values are more sensitive to the flow rate than to the saline solution concentration. Indeed, the conductivity curves are almost overlaid for 70 and 100 mL min^{-1} flow rates. For pH vs. time curves, phase I is less sensitive to the flow rate than phases II and III. The Cl^- and Na^+ final concentrations in the saline compartment are about $1.8\text{–}6.2 \times 10^{-4}$ mol L^{-1} which corresponds to 0.003–0.01 g L^{-1}.

To understand the effect of acidic and alkaline solution concentrations, a fourth set of experiments was realized at a flow rate of 70 mL min^{-1}, where the acidic and alkaline solution concentrations were different (see experiments 4.1 and 4.2 in Table 3).

The results displayed in Fig. 7(a) and (b) correspond to pH vs. time and conductivity of the saline solution vs. time, respectively.

A completely different behavior is noticed between these two experiments:

(1) For $C_A > C_B$, the phases II and III of the pH curves are absent even after 4 h of desalination. For the saline solution conductivity curves, the concavity is very pronounced with a great compensation time (approximately 2 h). This result confirms the competition between the desalination speed and the acidic solution leakage through the CEM.
(2) For $C_A < C_B$, the pH curve also includes three phases. However, in phase I, a rapid pH fluctuation is observed for few minutes (±5 min). This fluctuation is probably due to a higher alkaline concentration solution vs. acid concentration solution. Indeed, two phenomena co-exist during this phase:
    (a) A high alkaline concentration solution leads to an important OH^- diffusion to the saline compartment.
    (b) A high proton mobility.

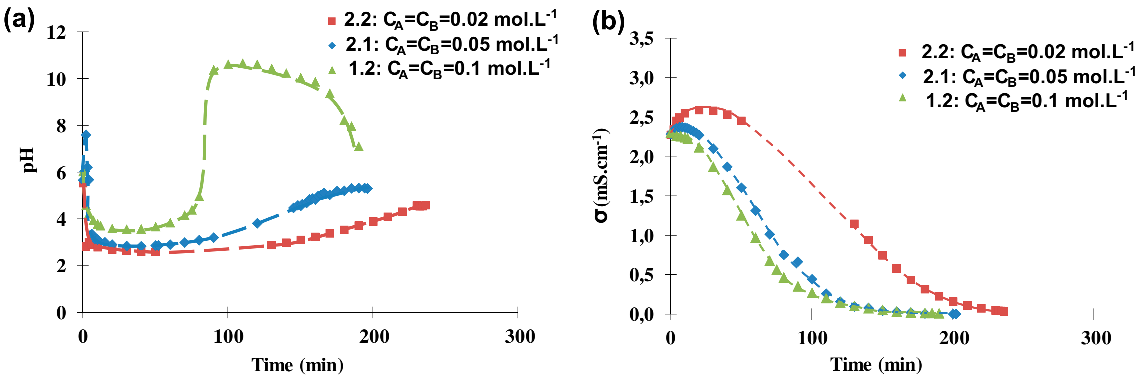

Fig. 5. Effects of the acidic and alkaline solution concentrations on pH vs. time (a) and saline solution conductivity vs. time (b) plots. The flow rate is maintained at 70 mL min^{-1}.

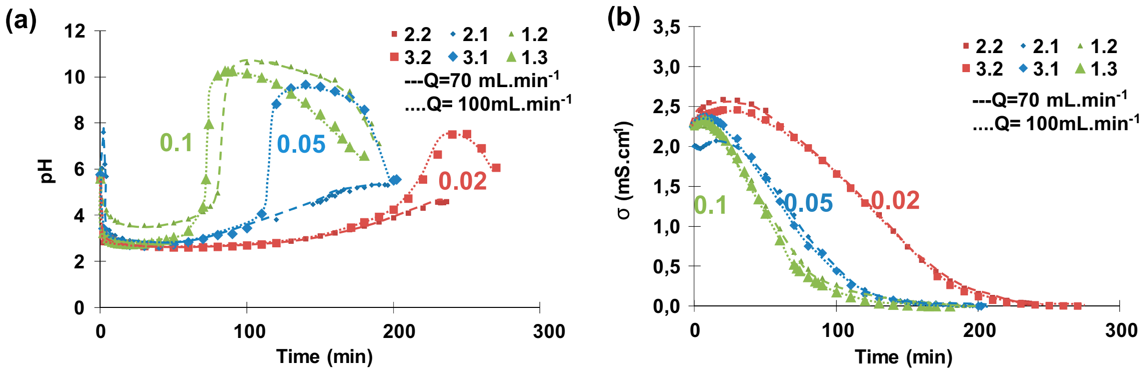

Fig. 6. Effects of the acidic and alkaline solution concentrations on pH vs. time (a) and saline solution conductivity vs. time (b) plots. The flow rate is maintained at 70 mL min^{-1} for 1.2, 2.1, 2.2 experiments and 100 mL min^{-1} for 1.3, 3.1, 3.2 experiments.

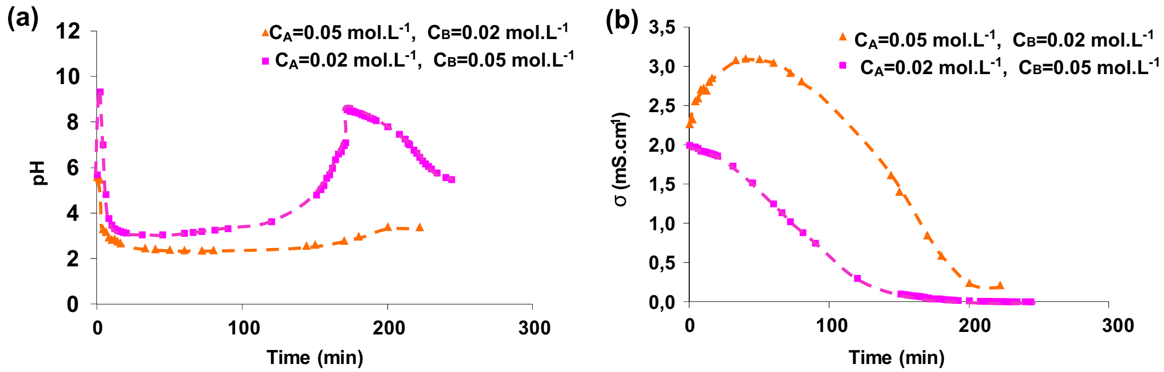

Fig. 7. Desalination experiments for different concentrations where $C_A \neq C_B$ at a constant flow rate (70 mL min^{-1}). Time dependence of pH (a) and conductivity in the saline compartment (b).

The compensation of these two phenomena causes a fluctuation.

Concerning the ionic conductivity, the saline solution conductivity curves do not present any visible concavity. Thus, the desalination speed is much faster than that obtained in the case in which $C_A > C_B$. The desalination speed and the neutral values of pH are achieved more rapidly when the acid and alkali solution concentrations are different from the saline solution concentration.

(3) Moreover, the amplitude of pH variation remains relatively low (from 3 to 8) compared to those obtained in the previous cases (from 3 to 10). Therefore, the speed of pH diminution in the third phase is rather fast up to initial pH value. The Cl^- and Na^+ final concentrations in the saline compartment are about $2.1–2.5 \times 10^{-4}$ mol L^{-1} (correspond to 0.01 g L^{-1}).

4. Conclusion

In this preliminary study on the use of ND for water demineralization, the effects of the flow rate and acidic/alkaline solution concentrations were investigated. The pH variation and the conductivity of the saline solutions were monitored.

We could establish that DBLs played a crucial role in the ion-exchange kinetics through the membranes.

The acidic and alkaline solution concentrations play a dominating role, particularly in the competition between the desalination speed and the HCl leakage through the CEM.

The shapes of the pH curves and the saline solution conductivity curves are clearly affected by the variations in the initial concentrations.

The desalination process was achieved in all the experiments (conductivity less than 0.25 mS cm^{-1}), but the time required to achieve this objective could be optimized, even though it was already satisfactory in certain experiments.

List of symbols

A — acid compartment
AEM — anion-exchange membrane
B — alkali compartment
C — saline compartment
C_A — acid concentration (mol L^{-1})
C_B — alkali concentration (mol L^{-1})
C_C — salt concentration in the saline solution (mol L^{-1})
CEM — cation-exchange membrane
DBLs — diffusion boundary layers
IEM — ion-exchange membrane
ND — neutralization dialysis
pH — pH value of the saline solution
Q — flow rate (mL min^{-1})
σ — saline solution conductivity (mS cm^{-1})

References

[1] K. Ghyselbrecht, M. Huygebaert, B. Van der Bruggen, Desalination of an industrial saline water with conventional and bipolar membrane electrodialysis, Desalination 318 (2013) 9–18.

[2] E.P. Gleem, T. Anday, R. Chaturvedi, Three halophytes for saline-water agriculture: An oilseed a forage and a gain crop, Environ. Exp. Bot. 92 (2013) 110–121.

[3] N.X. Tsiourtis, Desalination and the environment, Desalination 141 (2001) 223–236.

[4] J.V. Del Bene, G.H. Jirka, J. Largier, Ocean brine disposal, Desalination 97 (1994) 365–372.

[5] S. Dolnicar, A.I. Schäfer, Desalinated versus recycled water: Public perceptions and profiles of the accepters, J. Environ. Manage. 90 (2009) 888–900.

[6] H. Ben Bacha, Dynamic modeling and experimental validation of a water desalination prototype by solar energy using humidification dehumidification process, Desalination 322 (2013) 182–208.

[7] B. Tomaszewska, M. Bodzek, Desalination of geothermal waters using a hybrid UF-RO process. Part II: Membrane scaling after pilot-scale tests, Desalination 319 (2013) 107–114.

[8] A. Altaee, A. Mabrouk, K. Bourouni, A novel forward osmosis membrane pretreatment of seawater for thermal desalination processes, Desalination 326 (2013) 19–29.

[9] W. Li, W.B. Krantz, E.R. Cornelissen, A novel hybrid process of reverse electrodialysis and reverse osmosis for low energy seawater desalination and brine management, Appl. Energ. 104 (2013) 592–602.

[10] M. Igawa, K. Echizenya, T. Hayashita, M. Seno, Neutralization dialysis for deionization, Bull. Chem. Soc. Jpn. 60 (1987) 381–383.

[11] E.J. Parsi, Large electrodialysis stack development, Desalination 19 (1976) 139–151.

[12] K. Kusakari, F. Kawamata, N. Matsumoto, H. Saeki, Y. Terada, Electrodialysis plant at Hatsushima, Desalination 21 (1977) 45–50.

[13] S. Koga, Y. Mitsugami, Supply of potable water from brackish water by electro-dialysis desalination process at Ohoshima island in Tokyo prefecture, Ind. Water 239 (1978) 41–47.

[14] Y. Tanaka, Ion-exchange membrane electrodialysis program and its application to multi-stage continuous saline water desalination, Desalination 301 (2012) 10–25.

[15] AFNOR, Separation of ions in the liquid phase—Ion-exchange membranes polymers—Characteristics and test methods homopolar membranes, French standard NF X 45-200, 1995.

[16] R. Lteif, L. Dammak, C. Larchet, B. Auclair, Conductivité électrique membranaire: étude de l'effet de la concentration, de la nature de l'électrolyte et de la structure membranaire (Membrane electrical conductivity: A study of the effect of the concentration, the nature of the electrolyte and the membrane structure), Eur. Polym. J. 35 (1999) 1187–1195.

[17] L.V. Karpenko, O.A. Demina, G.A. Dvorkina, S.B. Parshikov, C. Larchet, B. Auclair, N.P. Berezina, Comparative study of methods used for the determination of electroconductivity of ion-exchange membranes, J. Electrochem. 37 (2001) 287–293.

[18] OMS, International standard of water quality and human health, Geneva, 1993.

[19] D. Mackay, P. Meares, On the correction for unstirred solution films in ion-exchange membrane cells, Kolloid Z. 167 (1959) 31–39.

[20] A. Dieye, Ph. D. thesis, Université Paris XII, 1995.

[21] M. Taky, G. Pourcelly, F. Lebon, C. Gavach, Polarization phenomena at the interfaces between an electrolyte solution and an ion exchange membrane, J. Electroanal. Chem. 336 (1992) 171–194.

[22] V. Tourreuil, L. Dammak, G. Bulvestre, B. Auclair, Dialysis applied to the selectivity study of cation exchange membranes in contact with strong electrolytes, New J. Chem., 22 (1998) 1463–1468.

[23] G.A. Denisov, G.A. Tishchenko, M. Bleha, L.K. Shataeva, Theoretical analysis of neutralization dialysis in the three-compartment membrane cell, J. Membr. Sci. 98 (1995) 13–25.